

Electronic Supplementary Material (ESI) for Materials Horizons.

This journal is © The Royal Society of Chemistry 2017

An 'Ideal' Universal Host for Highly Efficient Full-Color, White Phosphorescent and Thermally Activated Delayed Fluorescent OLEDs with Extremely Simple and Unified Structure

Kuo Gao,[†] Kunkun Liu,[†] Xiang-Long Li, Xinyi Cai, Dongjun Chen, Zhida Xu, Zuo Zheng He, Binbin Li,
Zhenyang Qiao, Dongcheng Chen, Yong Cao, Shi-Jian Su*

State Key Laboratory of Luminescent Materials and Devices and Institute of Polymer
Optoelectronic Materials and Devices, South China University of Technology, Guangzhou 510640,
China.

* Email: mssjsu@scut.edu.cn

[†] These two authors contributed equally to this work.

- ◆ **General information**
- ◆ **Device fabrication and characterization**
- ◆ **Materials synthesis**
- ◆ **Theoretical calculations**
- ◆ **Energy transfer calculations**
- ◆ **Figures**
- ◆ **¹H and ¹³C NMR spectra**
- ◆ **References**

General information. All the developed host materials were purified by silica gel chromatography and then by repeated thermal gradient vacuum sublimation before characterization and device fabrication. ^1H NMR spectra were recorded on a Bruker NMR spectrometer operating at 600 or 500 MHz, and ^{13}C NMR spectra were recorded at 150 MHz. TGA was performed on a Netzsch TG 209 under N_2 flow at a heating rate of $10\text{ }^\circ\text{C min}^{-1}$. DSC measurements were performed on a Netzsch DSC 209 under N_2 flow at a heating and cooling rate of $10\text{ }^\circ\text{C min}^{-1}$. UV-vis absorption spectra were recorded on a HP 8453 spectrophotometer. PL spectra were recorded on a Horiba Fluoromax-4 spectrofluorometer. CV was performed on a CHI600D electrochemical workstation using a platinum working electrode and a platinum wire counter electrode at a scanning rate of 100 mV s^{-1} against a Ag/AgCl (0.1 M AgNO_3 in acetonitrile) reference electrode using a nitrogen-saturated anhydrous acetonitrile and dichloromethane solution of 0.1 mol L^{-1} tetrabutylammonium hexafluorophosphate. PL quantum yields of the films were measured under air conditions by using an integrating sphere on a HAMAMATSU absolute PL quantum yield spectrometer C11347. Transient PL decay spectra were recorded using an Edinburgh FL920 fluorescence spectrophotometer. PL decays and the corresponding simultaneous PL spectra of the phosphorescent emitter-doped films were recorded at room temperature. The thin solid films used for absorption and PL spectral measurements were vacuum vapor deposited on quartz substrates.

Device fabrication and characterization. 95 nm indium tin oxide (ITO) coated glass substrates with a sheet resistance of $15\text{--}20\ \Omega\ \text{sq}^{-1}$ were subjected to a routine cleaning process of acetone, isopropyl alcohol, detergent, deionized water, and isopropyl alcohol under ultrasonic bath and treated with O_2 plasma for 20 mins. Organic layers and cathode were sequentially deposited on the ITO-coated glass substrates by thermal evaporation under high vacuum ($< 5 \times 10^{-4}\text{ Pa}$). And the deposition rates are $0.5\text{--}2\ \text{\AA s}^{-1}$ for organic layers, $0.1\ \text{\AA s}^{-1}$ for LiF layer and $5\text{--}6\ \text{\AA s}^{-1}$ for Al cathode, respectively. The current density-voltage-luminance (J-V-L) curves were detected by Keithley 2400 and Konica Minolta CS-200 electroluminescence measurement system. The electroluminescence (EL) spectrum was recorded using an optical analyzer Photo Research PR705 and power supply Keithley 2400. All the device characterizations were carried out at room temperature under ambient laboratory conditions.

All the electroluminescent devices are in a unified structure of ITO/TAPC (40 nm)/hosts: dopants (10 nm)/TmPyPB (40 nm)/LiF (1 nm)/Al (100 nm). The detailed structures of the devices are as follows.

Device B1: ITO/TAPC (40 nm)/m-DCz-S: 10 wt% Flr6 (10 nm)/TmPyPB (40 nm)/LiF (1 nm)/Al (100 nm);

Device B2: ITO/TAPC (40 nm)/S-DCz-ph: 10 wt% Flr6 (10 nm)/TmPyPB (40 nm)/LiF (1 nm)/Al (100 nm);

Device B3: ITO/TAPC (40 nm)/m-Cz-S: 10 wt% Flr6 (10 nm)/TmPyPB (40 nm)/LiF (1 nm)/Al (100 nm);

Device B4: ITO/TAPC (40 nm)/mCP: 10 wt% Flr6 (10 nm)/TmPyPB (40 nm)/LiF (1 nm)/Al (100 nm);

Device B5: ITO/TAPC (40 nm)/m-DCz-S: 6 wt% 2CzPN (10 nm)/TmPyPB (40 nm)/LiF (1 nm)/Al (100 nm);

Device G1: ITO/TAPC (40 nm)/m-DCz-S: 8 wt% Ir(ppy)₃ (10 nm)/TmPyPB (40 nm)/LiF (1 nm)/Al (100 nm);

Device G2: ITO/TAPC (40 nm)/m-DCz-S: 6 wt% ACRDSO2 (10 nm)/TmPyPB (40 nm)/LiF (1 nm)/Al (100 nm);

Device G3: ITO/TAPC (40 nm)/CBP: 6 wt% ACRDSO2 (10 nm)/TmPyPB (40 nm)/LiF (1 nm)/Al (100 nm);

Device O1: ITO/TAPC (40 nm)/m-DCz-S: 6 wt% Ir(bt)₂acac (10 nm)/TmPyPB (40 nm)/LiF (1 nm)/Al (100 nm);

Device O2: ITO/TAPC (40 nm)/m-DCz-S: 20 wt% Ir(dmppy)₂(dpp) (10 nm)/TmPyPB (40 nm)/LiF (1 nm)/Al (100 nm);

Device O3: ITO/TAPC (40 nm)/m-DCz-S: 6 wt% PO-01 (10 nm)/TmPyPB (40 nm)/LiF (1 nm)/Al (100 nm);

Device O4: ITO/TAPC (40 nm)/m-DCz-S: 6 wt% PyCN-ACR (10 nm)/TmPyPB (40 nm)/LiF (1 nm)/Al (100 nm);

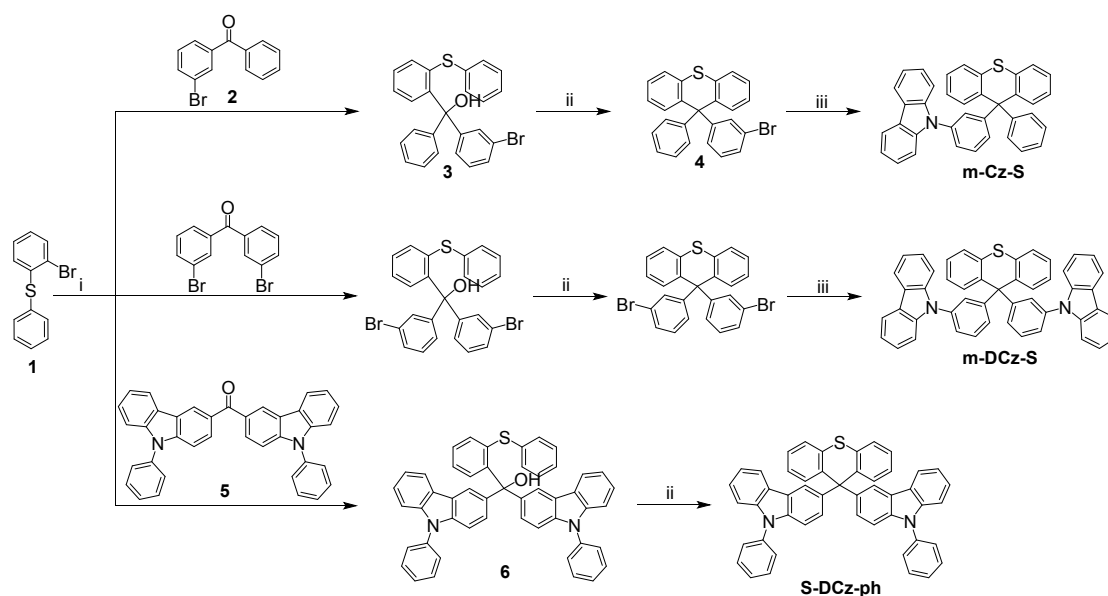
Device W1: ITO/TAPC (40 nm)/m-DCz-S: Flr6: PO-01 (100: 23: 0.8, 10 nm)/TmPyPB (40 nm)/LiF (1 nm)/Al (100 nm);

Device W2: ITO/TAPC (40 nm)/m-DCz-S: Flrpic: PO-01 (100: 23: 0.7, 10 nm)/TmPyPB (40 nm)/LiF (1 nm)/Al (100 nm);

Device W3: ITO/TAPC (40 nm)/m-DCz-S: Flr6: PyCN-ACR (100: 23: 1.3, 10 nm)/TmPyPB (40 nm)/LiF (1 nm)/Al (100 nm).

Hole only devices are in a structure of ITO/TAPC (40 nm)/hosts (10 nm)/TAPC (40 nm)/Al (100 nm), and electron only devices are in a structure of ITO/TmPyPB (40 nm)/hosts (10 nm)/TmPyPB (40 nm)/LiF (1 nm)/Al (100 nm).

Materials synthesis. All solvents and reagents were used as received from commercial suppliers without further purification. 2-Bromophenyl-phenyl-sulfane and m-DCz-S were synthesized according to literature.¹ Synthetic routes of the object compounds are outlined in Scheme S1.



Scheme S1. Molecular structures and synthetic routes of the 9,9-diphenyl-9H-thioxanthene derived compounds m-Cz-S, m-DCz-S and S-DCz-Ph. (i) n-BuLi (1 equiv), THF, -78 °C; (ii) AcOH, HCl, 80 °C, under N₂; (iii) carbazole, CuI, 18-crown-6, K₂CO₃, 1,3-dimethyl tetrahydropyrimidin-2(1H)-one (DMPU), 160 °C.

General coupling procedure for the synthesis of the host compounds.

(2-Bromophenyl)(phenyl)sulfane (**1**) (2.65 g, 10 mmol) was dissolved in dry tetrahydrofuran (THF) and degassed for 15 mins. The resulting mixture was cooled to -78 °C under nitrogen, and n-butyllithium

(2.5 M in hexanes) (4.5 mL, 11 mmol) was added in a dropwise manner. The resulting mixture was stirred at $-78\text{ }^{\circ}\text{C}$ for 1 h, and then ketone (10 mmol) in dry THF was added in one portion. After stirred overnight, brine (150 mL) was added, and the mixture was extracted with dichloromethane. The combined organic extracts were dried over anhydrous magnesium sulfate, filtered, and concentrated under reduced pressure.

9-(3-(9-phenyl-9H-thioxanthen-9-yl)phenyl)-9H-carbazole (m-Cz-S).

The general procedure for the synthesis of m-Cz-S was performed with (3-bromophenyl)(phenyl)methanone in 50 mL of dry THF as the ketone solution. A mixture of **3**, 50 mL acetic acid (AcOH), and 3 mL chloride acid was stirred under argon at $80\text{ }^{\circ}\text{C}$ for 3h. The reaction mixture was extracted with dichloromethane (DCM) and further purified by column chromatography using petroleum ether/ dichloromethane (3:1) as eluent to give a white solid (**4**) (3.04 g, total yield 60%). ^1H NMR (500 MHz, CDCl_3) δ 7.45 (dd, $J = 7.7, 1.3$ Hz, 2H), 7.40 (ddd, $J = 7.9, 1.9, 0.9$ Hz, 1H), 7.30 – 7.22 (m, 2H), 7.18 (td, $J = 7.7, 1.4$ Hz, 1H), 7.10 (t, $J = 7.9$ Hz, 5H), 6.95 – 6.88 (m, 3H), 6.81 – 6.74 (m, 2H), 6.71 (ddd, $J = 7.9, 1.8, 1.0$ Hz, 1H). **4** (0.608 g, 1.2 mmol), carbazole (0.44 g, 2.64 mmol), CuI (0.24 g), 18-crown-6 (0.33 g), K_2CO_3 (0.36 g), and 1,3-dimethyltetrahydropyrimidin-2(1H)-one (DMPU) (8 mL) were added to a 20 mL three-necked round-bottomed flask. The mixture was stirred and heated at $160\text{ }^{\circ}\text{C}$ for 24 h under a nitrogen atmosphere and then cooled to room temperature. The resulting mixture was extracted with DCM and dried over Na_2SO_4 , and then concentrated under vacuum. The residue was purified by column chromatography on silica gel using petroleum ether/ dichloromethane (3:1) as eluent to give a white solid (0.57 g, yield 71%). ^1H NMR (500 MHz, CDCl_3) δ 8.08 (d, $J = 7.7$ Hz, 2H), 7.55 – 7.47 (m, 3H), 7.44 (t, $J = 7.8$ Hz, 1H), 7.33 (ddd, $J = 8.2, 7.0, 1.2$ Hz, 2H), 7.29 (ddd, $J = 6.0, 3.7, 1.3$ Hz, 4H), 7.27 – 7.22 (m, 5H), 7.18 (td, $J = 7.7, 1.4$ Hz, 2H), 7.05 – 6.98 (m, 3H), 6.98 – 6.92 (m, 2H), 6.82 (ddd, $J = 7.8, 1.8, 1.2$ Hz, 1H). ^{13}C NMR (126 MHz, CDCl_3) δ 145.8, 143.7, 141.7, 140.3, 137.1, 133.7, 130.9, 129.2, 128.7, 127.85, 127.17, 126.7, 125.7, 124.6, 123.3, 120.1, 119.8, 109.7, 77.2, 77.0, 76.7, 61.7. MS (MALDI-TOF): m/z calcd for $\text{C}_{37}\text{H}_{25}\text{NS}$: 515.0905; found: 515.0905.

9,9'-((9H-Thioxanthen-9,9-diyl)bis(3,1-phenylene))bis(9H-carbazole) (m-DCz-S).

m-DCz-S (0.58 g, yield 70%) was synthesized as a white solid in a similar manner of m-Cz-S using bis(3-bromophenyl)ketone instead of **2**. ^1H NMR (500 MHz, CDCl_3 , δ , ppm): 8.11–8.02 (m, 4H), 7.53 (dd, $J = 7.7, 1.2$ Hz, 2H), 7.51–7.44 (m, 4H), 7.32–7.16 (m, 18H), 7.14 (dd, $J = 7.9, 1.1$ Hz, 2H), 6.96 (dt, $J = 7.2, 1.7$ Hz, 2H). ^{13}C NMR (126 MHz, CDCl_3 , δ , ppm): 145.6, 141.3, 140.3, 137.3, 133.7, 130.8, 129.2, 129.1, 129.1, 127.2, 126.9, 126.0, 125.8, 125.0, 123.3, 120.1, 119.9, 109.6, 61.7. MS (MALDI-TOF): m/z calcd for $\text{C}_{49}\text{H}_{32}\text{N}_2\text{S}$: 680.1343; found: 680.1343.

3,3'-(9H-thioxanthen-9,9-diyl)bis(9-phenyl-9H-carbazole)(S-DCz-Ph).

The general procedure for the synthesis of S-DCz-Ph was performed with bis(9-phenyl-9H-carbazol-3-yl)methanone in 50 mL of dry THF as the ketone solution. A mixture of **6**, 50 mL acetic acid (AcOH), and 3 mL chloride acid was stirred under argon at $80\text{ }^{\circ}\text{C}$ for 3h. The reaction mixture was extracted with DCM and further purified by column chromatography using petroleum ether/ dichloromethane (3:1) as eluent to give a white solid (3.04 g, total yield 60%). ^1H NMR (500 MHz, CDCl_3) δ 7.83 (d, $J = 7.8$ Hz, 1H), 7.62 – 7.54 (m, 4H), 7.52 (d, $J = 1.7$ Hz, 1H), 7.48 – 7.38 (m, 3H), 7.38 – 7.32 (m, 1H), 7.30 (d, $J = 8.7$ Hz, 1H), 7.28 – 7.24 (m, 2H), 7.21 – 7.08 (m, 3H), 6.95 (dd, $J = 8.7, 1.9$ Hz, 1H). ^{13}C NMR (126 MHz, CDCl_3) δ 143.2, 141.1, 139.5, 137.7, 136.9, 138.2, 131.6, 134.7, 138.2, 129.4, 218.3, 126.5, 133.0, 138.2, 127.1,

125.8, 125.5, 123.4, 122.5, 120.3, 119.7, 109.7, 108.8, 77.2, 77.0, 76.7, 61.8. MS (MALDI-TOF): m/z calcd for C₄₉H₃₂N₂S: 680.1343; found: 680.1343.

Theoretical calculations. Theoretical calculation of the compounds was carried out by using the Gaussian 09_B01 package. Density functional theory (DFT) calculation in the B3LYP/6-31G(d) basis set was performed to determine the ground state structure in the gas phase. Theoretical prediction for energy levels of the compounds was acquired based on the optimized structure. The M06-2x/6-31G(d) functional was utilized to gain insight into the character of the excited singlet states (S₁) and triplet states (T₁) by using the optimized structure mentioned above.

Energy transfer calculations. The rate of energy transfer k_{ET} from a donor to an acceptor and the efficiency of Förster energy transfer Φ_{ET} can be calculated as following equations:

$$k_{ET} = \frac{1}{\tau_D} \left(\frac{R_0}{R_{DA}} \right)^6$$

$$\Phi_{ET} = \frac{k_{ET}}{k_{ET} + \frac{1}{\tau_D}} = \frac{1}{1 + \left(\frac{R}{R_0} \right)^6}$$

Where τ_D is the decay time of the donor in the absence of acceptor, R_0 is the Förster radius and R_{DA} is the donor-to-acceptor distance. Among them, the Förster radius (R_0),² critical distance for the concentration quenching could be estimated by using the following equation:

$$R_0^6 = \frac{9000(\ln 10)\kappa^2\Phi_{PL}}{128\pi^5N_A n^4} \int_0^\infty F_D(\lambda)\varepsilon_A(\lambda)\lambda^4 d\lambda$$

where κ^2 is orientation factor (κ^2 is typically assumed to be 2/3 for the random orientation system), Φ_{PL} is the quantum yield of the donor in the absence of acceptor, N_A is Avogadro's number, n is the

refractive index of the medium, $\int_0^\infty F_D(\lambda)\varepsilon_A(\lambda)\lambda^4 d\lambda$ is the spectral overlap integral between donor PL [$F_D(\lambda)$] and acceptor absorption [$\varepsilon_A(\lambda)$] in which $F_D(\lambda)$ is the donor's fluorescence normalized by area, $\varepsilon_A(\lambda)$ is the molar decadic extinction coefficient of the acceptor and λ is the wavelength. And the distance between the donor and acceptor (R_{DA})³ can be calculated by using

$$R_{DA} = \left(N_G \times \frac{4\pi}{3} \right)^{-\frac{1}{3}}$$

where N_G is the quantity of guest molecules in a unit volume, which is in direct proportion to the guest doping concentration. According to Samuel's work,⁴ the density of chromophores can be described as $N_G = \beta \times \rho \times N_A/M_C$

where β is the fraction of guest present in the film, ρ is the density of the film (assumed to be 1 g cm⁻³), N_A is the Avogadro's number and M_C is the molecular weight of the guest. By using body-centered cubic structure stacking model, the average distance between guest molecules d_{AA} can be described as

$$d_{AA} = \sqrt[3]{\left(\frac{2}{w\%} \times 100\% \times \frac{4\pi r^3}{3} \right) / 68.02\% \times \frac{\sqrt{3}}{2}}$$

where $w\%$ is the weight percentage of guests, r is the radius of guest molecule (assumed to be 0.5 nm) and 68.02% is the accumulation factor of body-centered cubic structure.

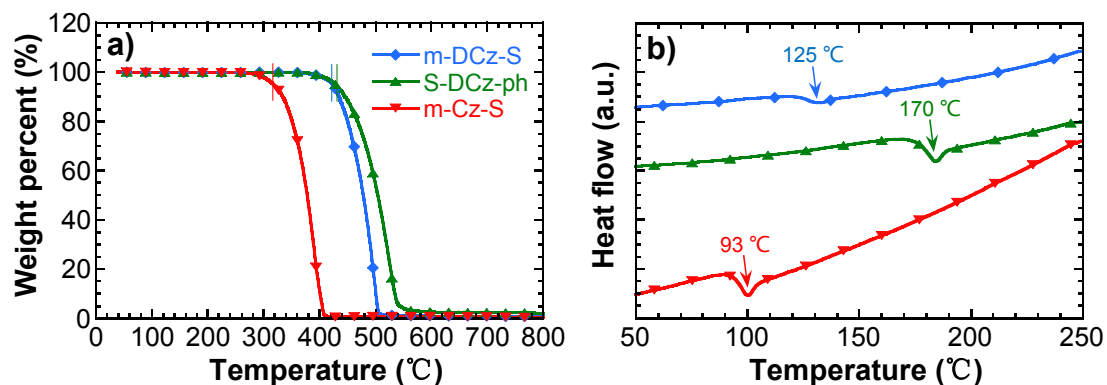


Figure S1. TGA a) and DSC b) curves of m-DCz-S, S-DCz-ph and m-Cz-S.

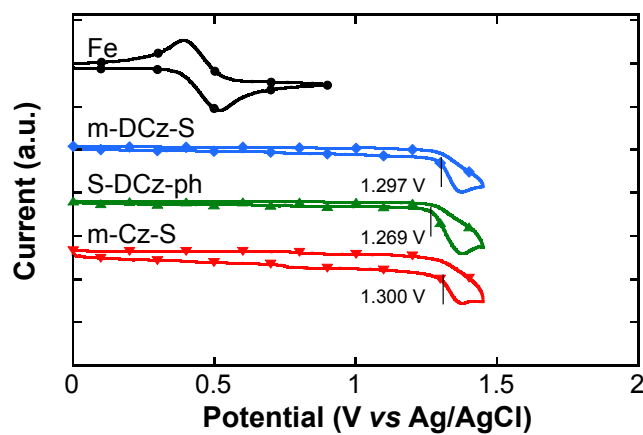


Figure S2. Cyclic voltammograms of m-DCz-S, S-DCz-ph and m-Cz-S measured in $\text{CH}_3\text{CN}/\text{DCM}$ (volume ratio: 1/4).

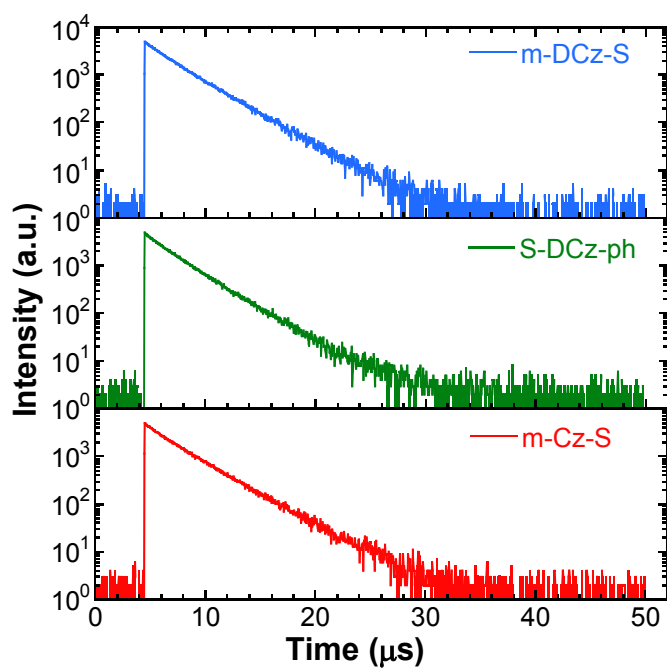


Figure S3. Transient PL decay curves of the co-deposited films of m-DCz-S: Flr6, S-DCz-ph: Flr6 and m-Cz-S: Flr6 with a doping concentration of 10 wt%.

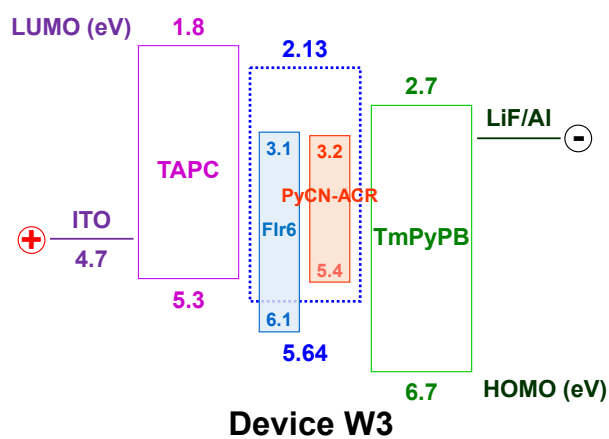
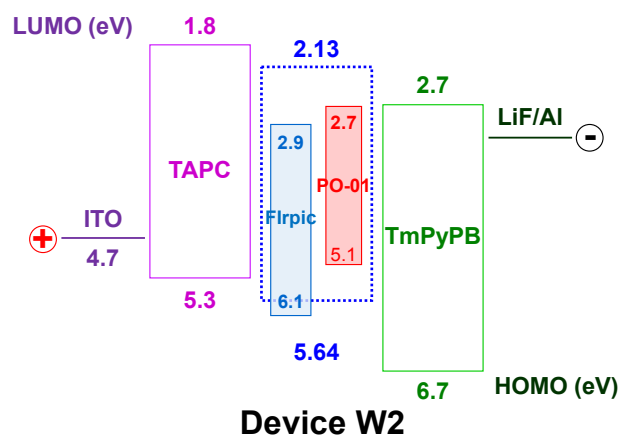
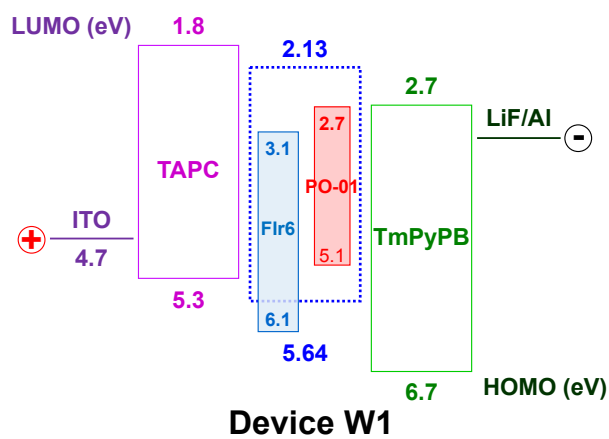


Figure S4. Energy level diagrams of devices W1, W2 and W3.

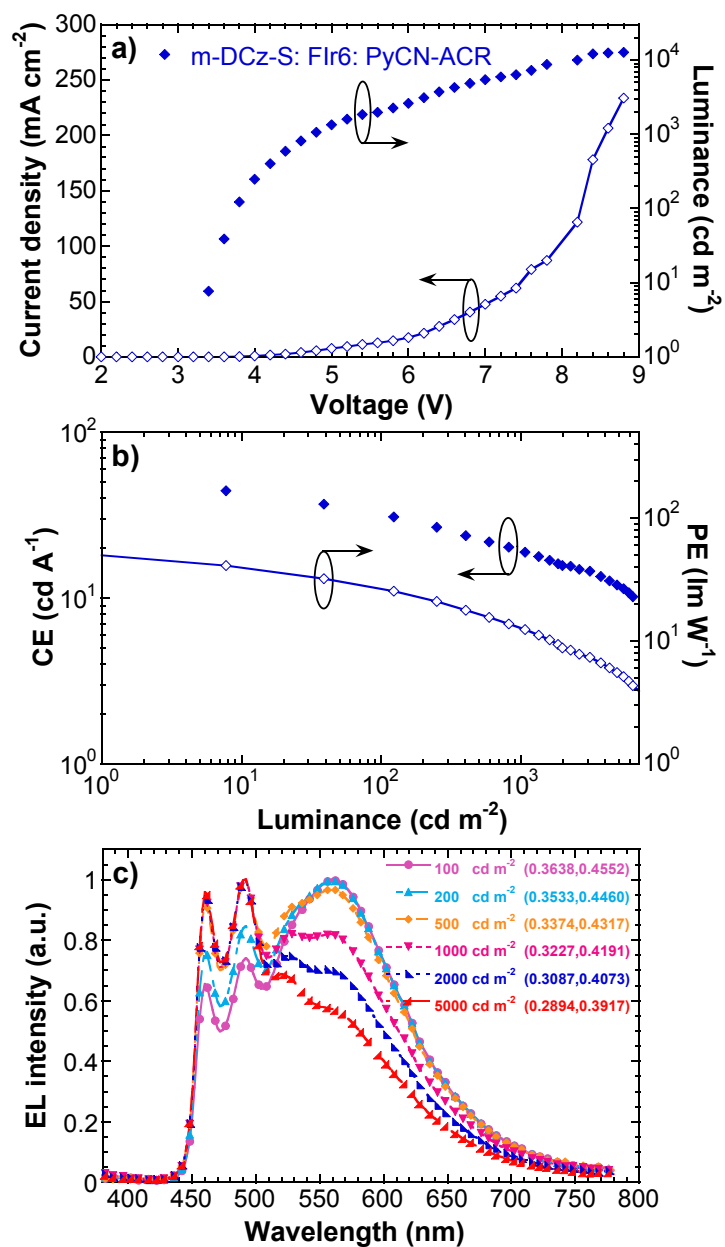
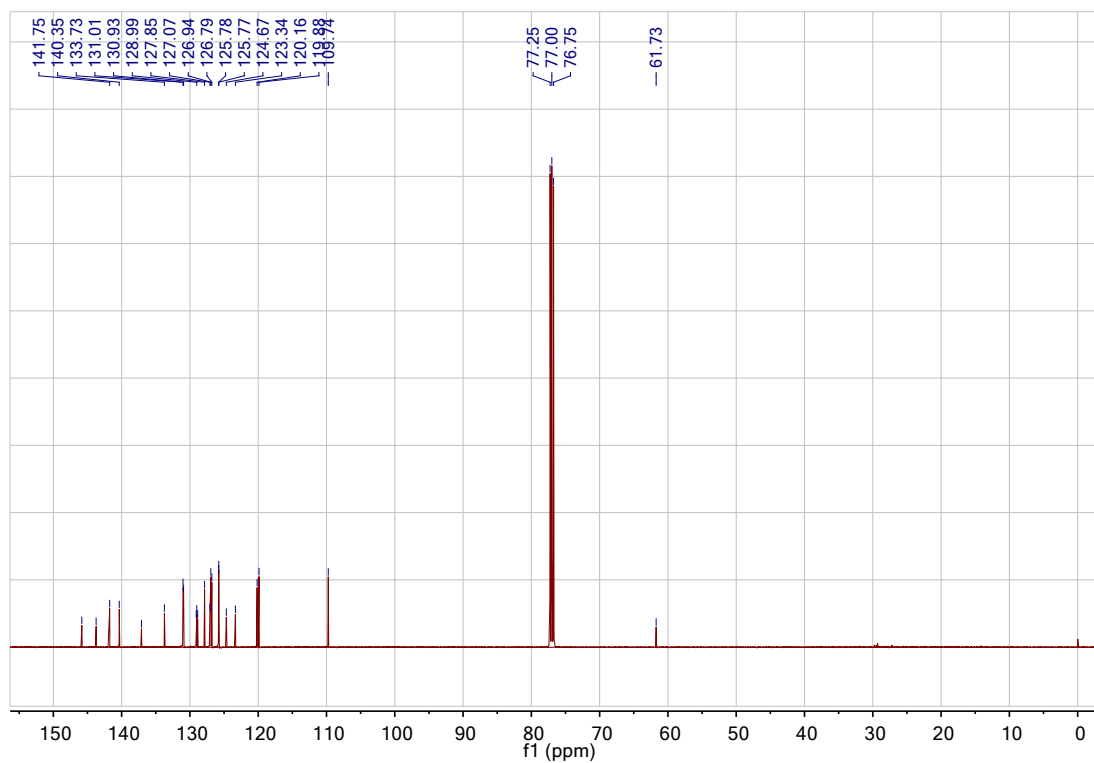
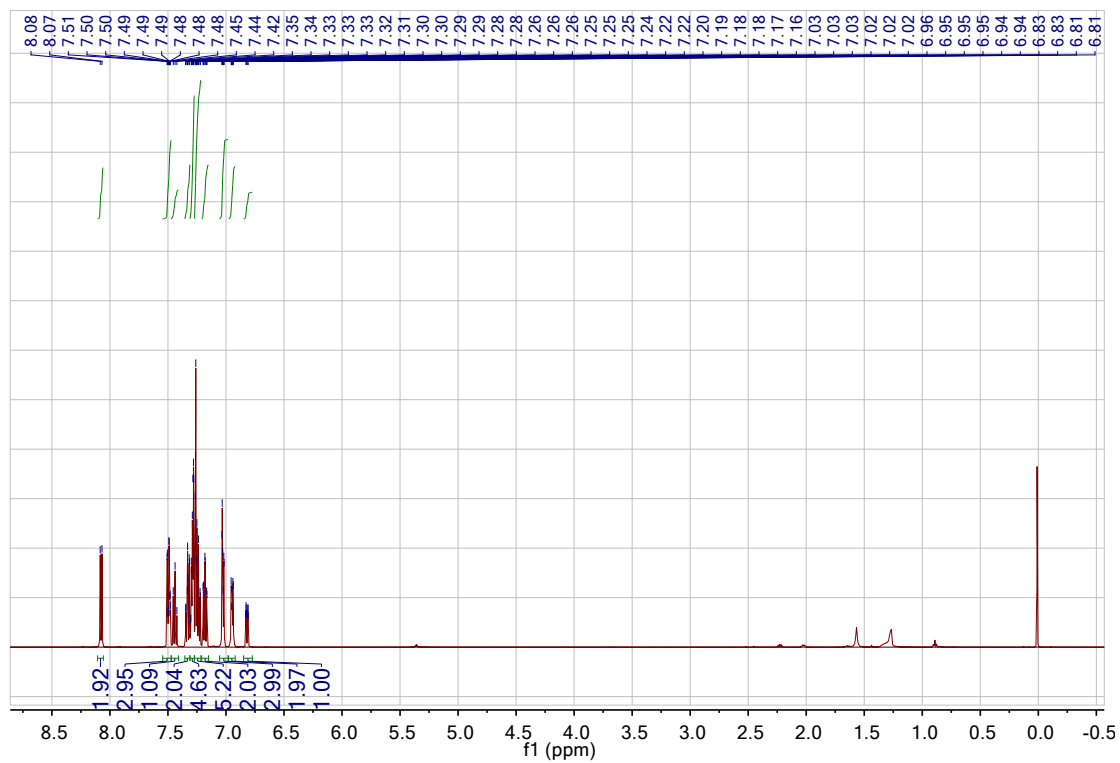


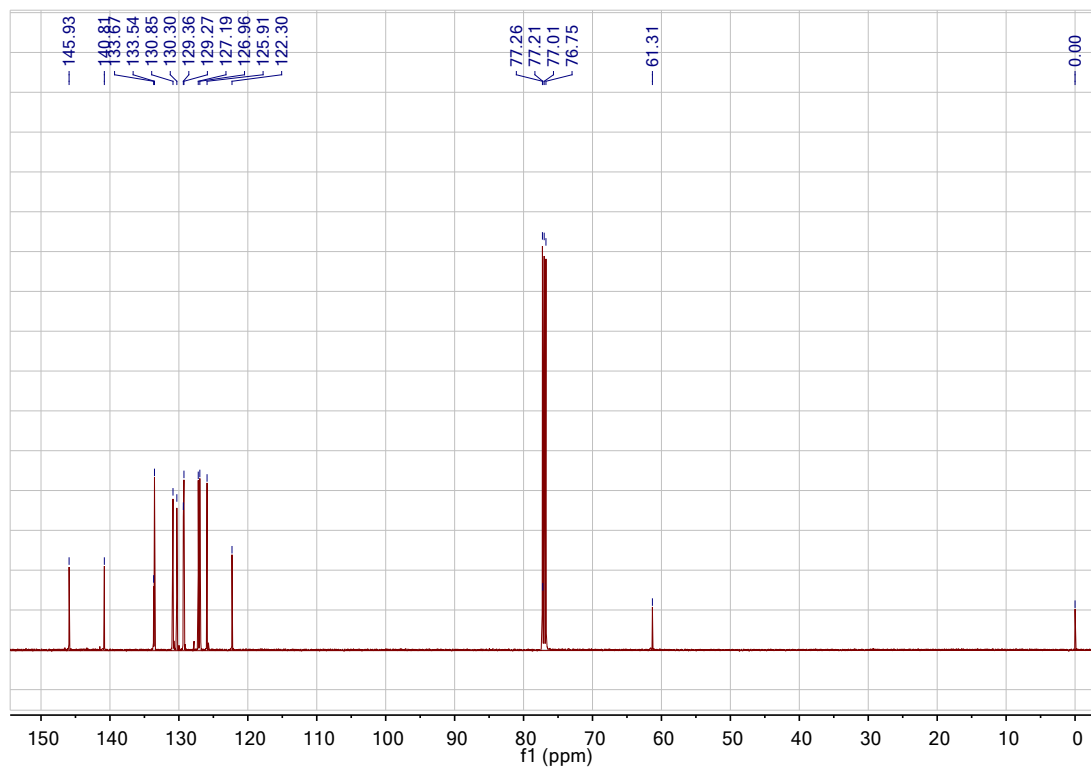
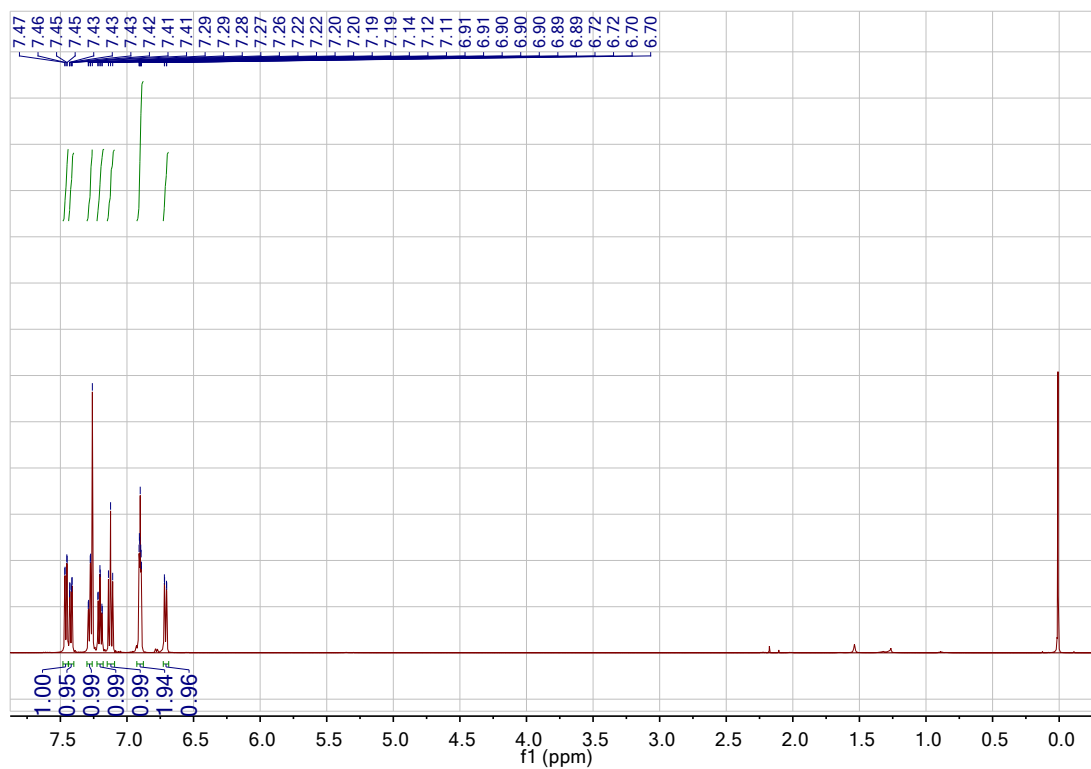
Figure S5. a) Current density-voltage-luminance (J-V-L), b) current efficiency-luminance-power efficiency (CE-L-PE), and c) electroluminescence (EL) spectra of device W3.

^1H and ^{13}C NMR spectra.

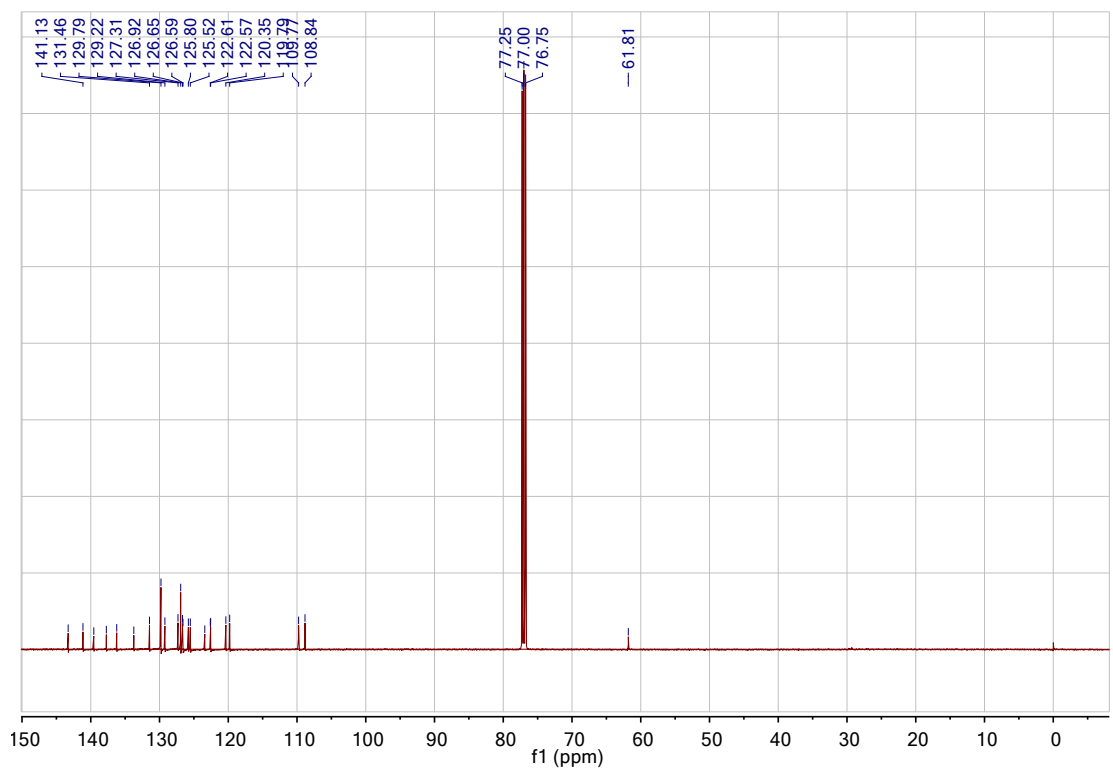
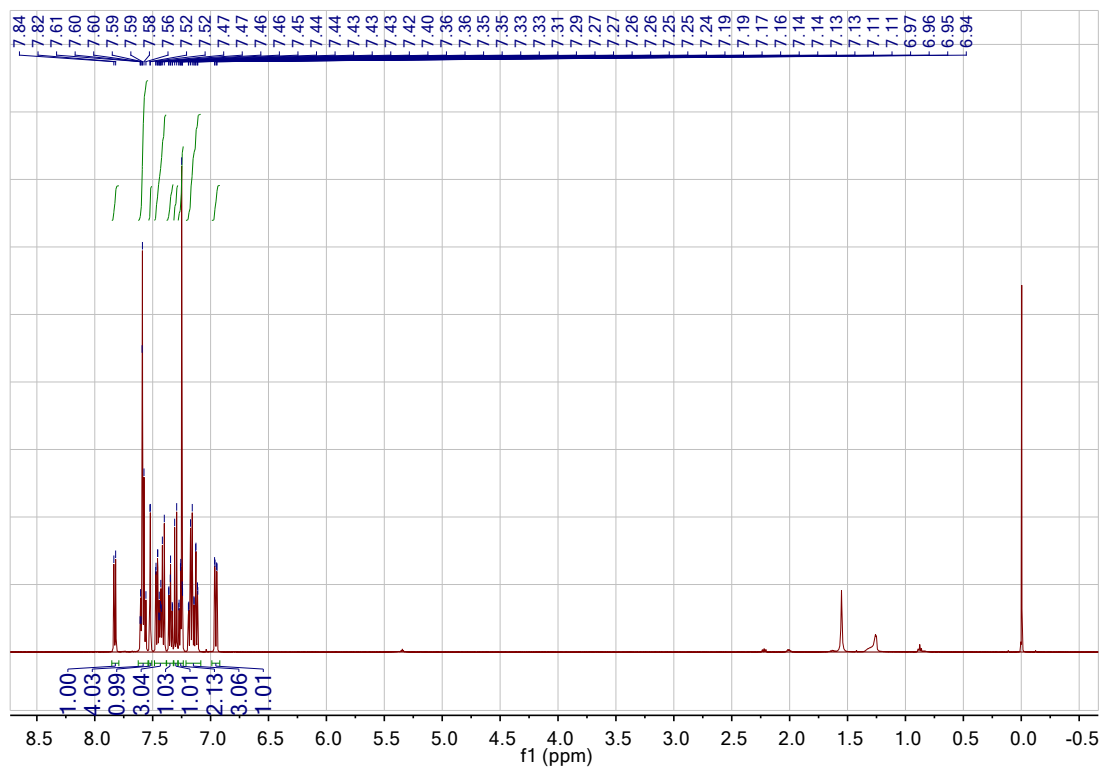
^1H and ^{13}C NMR spectra of m-Cz-S



^1H and ^{13}C NMR spectra of m-DCz-S



^1H and ^{13}C NMR spectra of S-DCz-Ph



References.

- 1 K. K. Liu, X. L. Li, M. Liu, D. C. Chen, X. Y. Cai, Y. C. Wu, C. C. Lo, A. Lien, Y. Cao and S. J. Su, *J. Mater. Chem. C*, 2015, **3**, 9999-10006.
- 2 W. S. Jeon, T. J. Park, S. Y. Kim, R. Pode, J. Jang and J. H. Kwon, *Org. Electron.*, 2009, **10**, 240-246.
- 3 H. Wang, B. Yue, Z. Xie, B. Gao, Y. Xu, L. Liu, H. Sun and Y. Ma, *Phys. Chem. Chem. Phys.*, 2013, **15**, 3527-3534.
- 4 P. E. Shaw, A. Ruseckas, J. Peet, G. C. Bazan and I. D. W. Samuel, *Adv. Funct. Mater.*, 2010, **20**, 155-161.